

# Excitonic magnetism in $d^6$ perovskites.

J. Fernández Afonso and J. Kuneš

*Institute of Solid State Physics, TU Wien  
Wiedner Hauptstrasse 8, 1040 Wien, Austria*

## **Abstract**

In this work we use the LDA+U method to study the possibility of exciton condensation in perovskites of transition metals with the  $d^6$  electronic configuration such as  $\text{LaCoO}_3$ . For realistic interaction parameters we find several distinct solutions exhibiting a spin-triplet exciton condensate, which gives rise to a local spin density distribution while the ordered moments are vanishingly small. Rhombohedral distortion from the ideal cubic structure suppresses the ordered state, contrary to the spin-orbit coupling which enhances the excitonic condensation energy. We explain the trends observed in the numerical simulations with the help of a simplified strong-coupling model. Our results indicate that  $\text{LaCoO}_3$  is close to the excitonic instability and suggest ways how to achieve the exciton condensation.



# First-principles study of electronic and mechanical properties in correlated electron system with the atomic number $Z=112$

Hana Čenčariková<sup>1</sup> and Dominik Legut<sup>2,\*</sup>

- 1) Institute of Experimental Physics, Slovak Academy of Sciences, Watsonova 47, 040 01 Košice, Slovakia
  - 2) Nanotechnology Centre & IT4Innovations Centre, VSB–Technical University of Ostrava, Czech Republic
- \*) dominik.legut@vsb.cz



## ABSTRACT

The first-principle calculations of the relativistic effects has been used to study the electrical and mechanical properties of the super-heavy element Copernicium. We have employed the single electron framework of the density functional theory including the Darwin term, mass-velocity and spin-orbit interaction to exhaustively analyze the phase stability of the five basic lattice structures body-centered cubic (*bcc*), face-centered cubic (*fcc*), simple cubic (*sc*), hexagonal closed packed (*hcp*) and rhombohedral (*rh*) one. It was found that the role of the spin-orbit coupling is crucial to compute the correct electronic structure of the ground-state, i.e. *bcc* structure instead of the *hcp* one, which is in accordance with Ref.[1], but in contradiction to Ref. [2]. It was observed, the all other structures are energetically less favorable than the *bcc* one. Further we determined mechanical properties (bulk modulus and elastic anisotropy) using calculated elastic constants for all structures. These also allow us to investigate the phase stability criteria that showed that Cn element can exist in two stable states corresponding to the *bcc* and surprisingly to the *sc* structure. Consequently, the pressure-induced structural phase transition between these two stable phases has been determined. In addition, it was found that the ground-state *bcc* structure exhibits the highest elastic anisotropy from single elements of the Periodic table. Finally, the analyzes of electronic properties of the Cn element support the experimental findings that the Copernicium is a metal.

## MOTIVATION & AIM

- What is the ground-state structure of Copernicium ( $Z=112$ )?
- What is the role of relativistic effects on phase stability?
- Is Copernicium metal or not?
- Are the predicted phases mechanically stable?

### Mechanical stability[5]:

- **cubic structures:**  $c_{11} - c_{12} > 0$ ,  $c_{11} + 2c_{12} > 0$ ,  $c_{44} > 0$
- **hcp structure:**  $c_{11} - |c_{12}| > 0$ ,  $c_{33}(c_{11} + c_{12}) - 2c_{12}^2 > 0$ ,  $c_{44} > 0$
- **rh structure:**  $c_{11} - |c_{12}| > 0$ ,  $c_{33}(c_{11} + c_{12}) - 2c_{12}^2 > 0$ ,  $c_{44}(c_{11} - c_{12}) - 2c_{12}^2 > 0$ ,  $c_{44} > 0$
- $c' = \frac{c_{11} - c_{12}}{2}$ , and  $A = c_{44}/c'$ [6], for  $A = 1$  isotropic behavior[7]

## RESULTS: Effect of relativity taken into the calculations

### Non-relativistic (NR):

	$a$ [a.u.]	$c$ [a.u.]	$\Delta E$ [mRy/at.]	$V_{at.}$ [a.u. <sup>3</sup> ]	$B$ [GPa]	$c_{ij}$ [GPa]
<b>fcc (S)</b>	9.4356		1.1	210 $A = 2.33$	47	$c_{11} = 47.4$ $c_{12} = 47.2$ $c_{44} = 0.2$
<b>bcc (U)</b>	7.5190		5.9	213 $A = -0.17$	45	$c_{11} = 29$ $c_{12} = 53$ $c_{44} = 2(2)$
<b>sc (U)</b>	6.2762		18.7	247 $A = -0.26$	33	$c_{11} = 64$ $c_{12} = 17$ $c_{44} = -6$
<b>hcp (S)</b>	6.5184	11.3365	0	209	48	$c_{11} = 89$ $c_{12} = 36$ $c_{13} = 35$ $c_{33} = 54$ $c_{55} = 24$
<b>rh (U)</b>	7.5649	86.8°	6.8	215	50	$c_{11} = 58$ $c_{12} = 43$ $c_{13} = 47$ $c_{44} = 1$ $c_{33} = 38$ $c_{44} = -7$

### Scalar-relativistic (SR):

	$a$ [a.u.]	$c$ [a.u.]	$\Delta E$ [mRy/at.]	$V_{at.}$ [a.u. <sup>3</sup> ]	$B$ [GPa]	$c_{ij}$ [GPa]
<b>fcc (U)</b>	9.1080		0.1	189 $A = -52$	35	$c_{11} = 34.5$ $c_{12} = 35.0$ $c_{44} = 13$
<b>bcc (U)</b>	7.2443		1.0	190 $A = -17$	34	$c_{11} = 33$ $c_{12} = 35$ $c_{44} = 17$
<b>sc (U)</b>	6.0901		9.9	226 $A = -0.07$	22	$c_{11} = 57$ $c_{12} = 4$ $c_{44} = -2$
<b>hcp (S)</b>	6.44297	10.4847	0	188	35	$c_{11} = 49$ $c_{12} = 29$ $c_{13} = 27$ $c_{33} = 52$ $c_{55} = 7$
<b>rh (S)</b>	7.2930	88.8°	2.1	194	32	$c_{11} = 49$ $c_{12} = 27$ $c_{13} = 20$ $c_{44} = 0.02$ $c_{33} = 51$ $c_{44} = 4$

### SR with spin-orbit coupling (SOC):

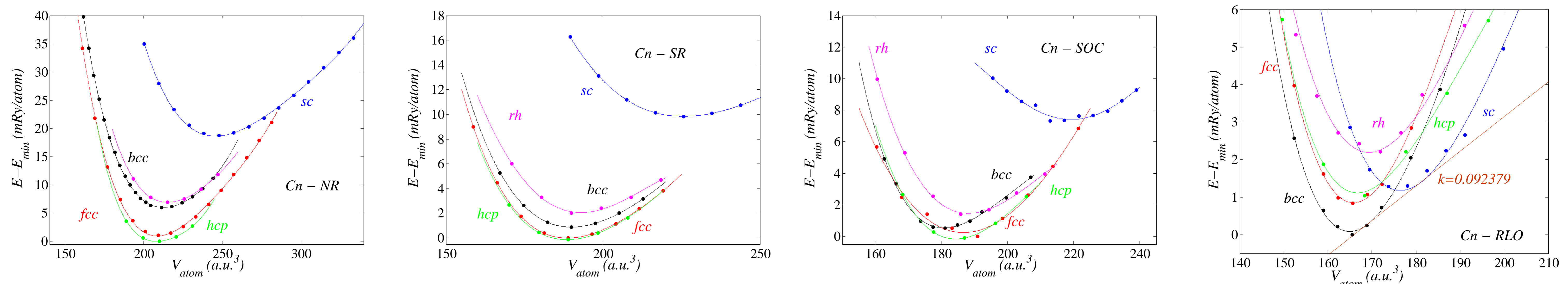
	$a$ [a.u.]	$c$ [a.u.]	$\Delta E$ [mRy/at.]	$V_{at.}$ [a.u. <sup>3</sup> ]	$B$ [GPa]	$c_{ij}$ [GPa]
<b>fcc (U)</b>	9.0726		0.40	187 $A = 0.57$	38	$c_{11} = 15$ $c_{12} = 50$ $c_{44} = -10$
<b>bcc (U)</b>	7.1243		0.69	181 $A = -4$	47	$c_{11} = 28$ $c_{12} = 57$ $c_{44} = 58$
<b>sc (U)</b>	6.0326		7.53	220 $A = -0.02$	32	$c_{11} = 70$ $c_{12} = 13$ $c_{44} = -0.59$
<b>hcp (S)</b>	6.4097	10.3624	0	184	14	$c_{11} = 62$ $c_{12} = 42$ $c_{13} = -58$ $c_{33} = 150$ $c_{55} = 24$
<b>rh (U)</b>	7.2232	88.5°	1.62	188	38	$c_{11} = 72$ $c_{12} = 72$ $c_{13} = 13$ $c_{44} = -4$ $c_{33} = 45$ $c_{44} = 3$

### SOC + rel. local basis (RLO):

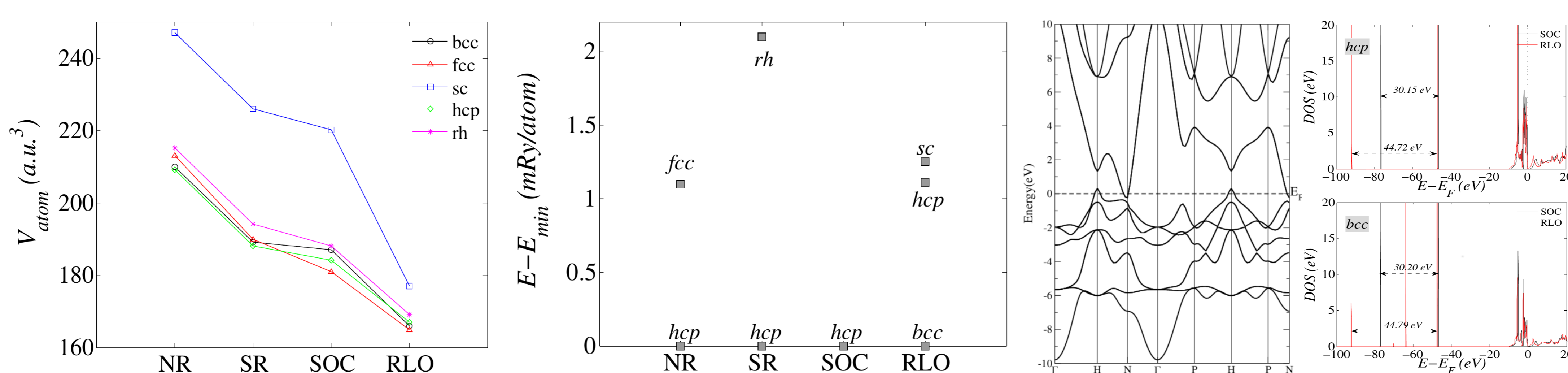
	$a$ [a.u.]	$c$ [a.u.]	$\Delta E$ [mRy/at.]	$V_{at.}$ [a.u. <sup>3</sup> ]	$B$ [GPa]	$c_{ij}$ [GPa]
<b>fcc (U)</b>	8.7214		0.93	166 $A = -14.4$	63	$c_{11} = 60$ $c_{12} = 65$ $c_{44} = 36$
<b>bcc (S)</b>	6.9118		0	165 $A = 9.75$	62	$c_{11} = 67$ $c_{12} = 59$ $c_{44} = 39$
<b>sc (S)</b>	5.6120		1.25	177 $A = 0.42$	54	$c_{11} = 63$ $c_{12} = 49$ $c_{44} = 3$
<b>hcp (S)</b>	6.1781	10.0889	1.11	167	45	$c_{11} = 70$ $c_{12} = 56$ $c_{13} = 27$ $c_{33} = 59$ $c_{55} = 15$
<b>rh (U)</b>	6.9911	$\alpha = 85.5^\circ$	2.19	169	56	$c_{11} = 45$ $c_{12} = 14$ $c_{13} = 82$ $c_{44} = 9$ $c_{33} = 40$ $c_{44} = -0.02$

where the (U) and (S) states for the UNSTABLE and STABLE phase, i.e. not-filling/filling the conditions of mechanical stability[5, 7].

## RESULTS: Energy vs. volume for investigated structures along the increase of relativistic effects



## RESULTS: volume and stable phases vs. relativity, E vs. volume for RLO, bandstructure and DOS of bcc and hcp of Cn (SOC vs. RLO)



## CONCLUSION

- Ground-state of Cn is *bcc* structure (by 1mRy/at over *hcp* one)
- relativistic effects act as pressure
- Possible *sc*→*bcc* phase transition
- Cn in *bcc* structure is a metal in accord with exp.[17]
- *bcc* Cn has unusually high elastic anisotropy  $A = 9.75$ , i.e. higher than Li ( $A = 8.52$ ) and on the opposite bound of  $A$  as being for *sc* Po ( $A = 0.06$ )[16]

## Computational details

- WIEN2k code [8], local density approximation (LDA) [9],  $R_{MT}K_{MAX}=15$ ,  $R_{MT}(Cn)=2.4$  a.u.,  $l_{max}=12$ , k-points grid  $19 \times 19 \times 19$  mesh, core electrons  $[Xe]4f^{14}, 5d^{10}, 6s^2$  are treated by Dirac approach [10], SOC treated within the second-variation method [11] with energy  $E_{cut}=6$  Ry, additional local orbitals for the *p* semi-core states, where the radial part of the  $p_{1/2}$  basis is obtained as of the Dirac equations for  $l = 1$  and  $j = \frac{1}{2}$  [12, 13] (RLO).
- Elastic constants  $c_{ij}$  obtained from total energy vs deformations along ELAST and IREALST packages [14, 15] with evaluations done third order fit.

## Acknowledgement

This work was supported by The Ministry of Education, Youth and Sports from the Large Infrastructures for Research, Experimental Development and Innovations project IT4Innovations National Supercomputing Center LM2015070 and by the grant No. 17-27790S of the Grant Agency of the Czech Republic and by The Ministry of Education, Youth and Sports from the National Programme of Sustainability (NPU II) project "IT4Innovations excellence in science - LQ1602" and Mobility grant No. MB7847811 and Student Grant Competitions of VSB-TU Ostrava (SP2017/184). H.C. acknowledges support by the Slovak Research and Development Agency (APVV) under Grant No. DS-2016-0046. The financial support provided by VEGA under Grant No. 1/0043/16 is also gratefully acknowledged.

## References

- [1] A. Zaoui and M. Ferhat, Sol. Stat. Commun. **152** (2012) 530.
- [2] R. Atta-Fynn and A. K. Ray, Sol. Stat. Commun. **201** (2015) 88.
- [3] N. Gaston, I. Opahle, H. W. Gaggeler, and P. Schwerdtfeger, Angew. Chem. Int. Ed. **46** (2007) 1663.
- [4] D. A. Papaconstantopoulos, Handbook of the Band Structure of Elemental Solids From  $Z = 104$  To  $Z = 112$ , Springer Science+Business Media New York 2015.
- [5] F. Mouhat and F. X. Coudert, Phys. Rev. B **90** (2014) 224104.
- [6] C. Zener, Elasticity and Anelasticity of Metals, University of Chicago Press, Chicago, IL, 1948.
- [7] G. Grimvall, Thermophysical Properties of Materials, Amsterdam: Elsevier 1999.
- [8] P. Blaha, K. Schwarz, and J. Luitz, WIEN2K, Vienna, University of Technology, 1997.
- [9] J. P. Perdew and Y. Wang, Phys. Rev. B **45** (1992) 13244.
- [10] J. P. Desclaux, Comp. Phys. Comm. **1** (1975) 216.
- [11] D. D. Koelling and B. N. Harmon, J. Phys. C **10** (1977) 3107.
- [12] J. Kuneš, P. Novák, R. Schmid, P. Blaha, and K. Schwarz, Phys. Rev. B **64** (2001) 153102.
- [13] D. J. Singh, Phys. Rev. B **43** (1991) 6388.
- [14] T. Charpin, Lab. Geomatériaux de IIPGP, Paris, France. Modified by F. Karsai, Inst. for Mater. Chem. TU Vienna.
- [15] M. Jamal, Ghods City-Tehran, Iran.
- [16] D. Legut, M. Friák and M. Šob, Phys. Rev. Lett. **99** (2007) 016402.
- [17] A. Yakushev et al., Inorg. Chem. **53** (2014) 1624.



# Effect of high-valent metal-ion doping on the properties of NCM-523 Li-ion battery materials

Arup Chakraborty, Boris Markovsky, Doron Aurbach, Dan T. Major

Chemistry Department, Bar-Ilan University, Ramat Gan 52900, Israel

**Abstract:** In recent years, rechargeable Li-ion batteries have received immense attention as these materials are among the most promising candidates as renewable energy alternatives.[1,2]  $\text{LiNi}_{1-x-y}\text{Co}_x\text{Mn}_y\text{O}_2$  is arguably the most important of currently available cathode materials for Li-ion battery due to their stability and high operating voltage.[3,4] In these materials, there are various challenging issues like stability, capacity fading etc.[5] In this work, we show that the performance of  $\text{LiNi}_{0.5}\text{Co}_{0.2}\text{Mn}_{0.3}\text{O}_2$  (NCM-523) can be improved by 1% doping by the high-valent metal ion, Mo. We perform density functional theory calculations to study the most favourable doping site in NCM-523. We find that replacing Ni with Mo is the most favourable process, possibly due to the similar ionic radius of  $\text{Mo}^{6+}$  and  $\text{Ni}^{3+}$ . We also observe that the average Ni-O bond length is slightly larger in the case of Mo-doped NCM-523, compared to the undoped system, in agreement with XANES experiment. Further, it is observed that there is an increase in  $\text{Ni}^{2+}$  ions and a concomitant decrease in  $\text{Ni}^{3+}$  ions due to Mo-doping. This change in oxidation states is ascribed to a charge-compensation effect.

**Keywords:** Li-ion battery, DFT, doping, NCM cathode materials.

## References:

1. J.-M. Tarascon and M. Armand, *Nature*, 414, 359 (2001).
2. M. Saiful Islam and C. A. J. Fisher, *Chem. Soc. Rev.*, 43, 185 (2014).
3. M. Dixit, M. Kosa, O. S. Lavi, B. Markovsky, D. Aurbach and D. T. Major, *Phys.Chem.Chem.Phys.*, 18, 6799 (2016).
4. F. Schipper, E. M. Erickson, C. Erk, J. Y. Shin, F. F. Chesneau, and D. Aurbach, *Journal of The Electrochemical Society*, 164 (1) A6220 (2017).
5. F. Schipper, M. Dixit, D. Kovacheva, M. Talianker, O. Haik, J. Grinblat, E. M. Erickson, C. Ghanty, D. T. Major, B. Markovsky and D. Aurbach, *J. Mater. Chem. A*, 4,16073 (2016).

# Nature of the structural transition in $\text{Er}_5\text{Si}_4$

R. M. Costa<sup>1</sup>, J. H. Belo<sup>1</sup>, M. Barbosa<sup>1</sup>, J. P. Araújo<sup>1</sup> and A. M. Pereira<sup>1</sup>

<sup>1</sup>*IFIMUP and IN-Institute of Nanoscience and Nanotechnology, Departamento de Física e Astronomia, Faculdade de Ciências, Universidade do Porto, Rua do Campo Alegre, 687, 4169-007 Porto, Portugal*

**Abstract:** In the last few years, magnetocaloric materials have received a lot of attention due to their potential in the cooling industry, as well as their importance for academic research. Several materials exhibiting giant magnetocaloric effect (GMCE) were discovered, most notably the  $\text{R}_5(\text{Si},\text{Ge})_4$  family (where R = rare earth element), which has a wide range of compounds presenting distinct properties among themselves. In particular, the  $\text{Er}_5\text{Si}_4$ , is an interesting case to study because it shows an apparent (de)coupling between the magnetic and crystal structure and a purely structural transition that can only be accomplished at relatively high magnetic fields. It is also the only element of the family that shows the reversible martensitic-like distortion from orthorhombic to monoclinic on cooling. In this work, a thermodynamic model, with the aid of first principles simulations, aims to explain the reversible magnetic-field-induced structural transition of  $\text{Er}_5\text{Si}_4$ .

---

## References and links

1. Y. Mudryk, N. K. Singh, V. K. Pecharsky, D. L. Schlagel, T. A. Lograsso, and K. A. Gschneidner, "Magnetic and structural properties of single-crystalline  $\text{Er}_5\text{Si}_4$ ," *Physical Review B* **85**(9), 94432 (2012).
  2. Gordon J. Miller, "Complex rare-earth tetrelides,  $\text{RE}_5(\text{Si}_x\text{Ge}_{1-x})_4$ : New materials for magnetic refrigeration and a superb playground for solid state chemistry," *Chemistry Society Reviews* **35**(9), 799 (2006).
  3. V. K. Pecharsky, A. O. Pecharsky, Yu Mozharivskij, K. A. Gschneidner Jr., and G. J. Miller, "Decoupling of the Magnetic and Structural Transformations in  $\text{Er}_5\text{Si}_4$ ," *Physical Review Letters* **91**(20), 207205 (2003).
  4. C. Magen, C. Ritter, L. Morellon, P. A. Algarabel, M. R. Ibarra, A. O. Tsokol, K. A. Gschneidner Jr., and V. K. Pecharsky, "Magnetic-field-induced structural transformation in  $\text{Er}_5\text{Si}_4$ ," *Physical Review B* **74**(17), 174413 (2006).
  5. A. M. Pereira, J. P. Araújo, M. E. Braga, R. P. Pinto, J. Ventura, F. C. Correia, J. M. Teixeira, J. B. Sousa, C. Magen, P. A. Algarabel, et al, "Transport and magnetic properties of the  $\text{Er}_5\text{Si}_4$  compound," *Journal of Alloys and Compounds* **423**(1), 66 (2006).
  6. V. Franco, J. S. Blázquez, B. Ingale, and A. Conde, "The magnetocaloric effect and magnetic refrigeration near room temperature: materials and models," *Materials Research* **42**(1), 305 (2012).
-

# Electric field gradients at $^{181}\text{Ta}$ probe in $\text{Zr}_7\text{Ni}_{10}$ and $\text{Hf}_7\text{Ni}_{10}$ intermetallic binary alloys; investigations by time-differential perturbed angular correlation spectroscopy

Sourav Kumar Dey,<sup>1</sup> Chandi Charan Dey,<sup>1</sup> and Satyajit Saha<sup>1</sup>

<sup>1</sup>*Saha Institute of Nuclear Physics, HBNI,  
1/AF, Bidhannagar, Kolkata - 700064, India.*

## Abstract

Intermetallic compounds of  $\text{Zr}_7\text{Ni}_{10}$  and  $\text{Hf}_7\text{Ni}_{10}$  have been studied by perturbed angular correlation (PAC) spectroscopy considering their important technological applications. In both these samples, production of multiple phases have been observed. In  $\text{Zr}_7\text{Ni}_{10}$ , four quadrupole frequencies have been found at room temperature. The predominant component ( $\sim 41\%$ ) with values of  $\omega_Q = 72.8(2)$  Mrad/s,  $\eta = 0$ ,  $\delta = 1.6(6)\%$  has been attributed to  $\text{ZrNi}_3$  phase. The second major component ( $\sim 29\%$ ) with values of  $\omega_Q = 58.5(3)$  Mrad/s,  $\eta = 0.73(1)$ ,  $\delta = 0$  is tentatively assigned to  $\text{Zr}_7\text{Ni}_{10}$  phase. Additional minor phase ( $\sim 12\%$ ) with values of  $\omega_Q = 77.4(7)$  Mrad/s,  $\eta = 0.81(2)$  and  $\delta = 0$  has been identified as  $\text{Zr}_8\text{Ni}_{21}$ . In  $\text{Hf}_7\text{Ni}_{10}$ , similar values of quadrupole frequency at room temperature has been found which indicate its iso-structurality with  $\text{Zr}_7\text{Ni}_{10}$ . The main component ( $\sim 68\%$ ) with values of  $\omega_Q = 72.4(4)$  Mrad/s,  $\eta = 0$  and  $\delta = 7(1)\%$  has been attributed to  $\text{HfNi}_3$ . The second minor phase ( $\sim 11\%$ ) with values of  $\omega_Q = 56.9(6)$  Mrad/s and  $\eta = 0.84(3)$  is assigned to  $\text{Hf}_7\text{Ni}_{10}$ . Temperature dependent PAC measurements have been carried out in these alloys in the temperature range 77-973 K to observe any structural and compositional changes in the sample. The sample  $\text{Zr}_7\text{Ni}_{10}$  has also been characterized by X-ray powder diffraction (XRD) measurements. From the analysis of the XRD spectrum, production of  $\text{Zr}_7\text{Ni}_{10}$  phase has been confirmed. In addition, ab-initio calculations using the augmented plane wave plus local orbitals (APW+lo) method, within the framework of the density functional theory (DFT) will be performed to compare with experimental results in both the compounds to assign the quadrupole frequency components.

## Structure and Dynamics of Main-Group Halide Perovskite Photovoltaics

Douglas H. Fabini,<sup>a,b</sup> Geneva Laurita,<sup>b</sup> Emily C. Schueller,<sup>a,b</sup> Constantinos C. Stoumpos,<sup>c</sup>  
Ting-Ann Siaw,<sup>d</sup> Songi Han,<sup>d</sup> Mercouri G. Kanatzidis,<sup>c</sup> and Ram Seshadri<sup>a,b,c</sup>

<sup>a</sup>Materials Research Laboratory, University of California, Santa Barbara, CA 93106, United States

<sup>b</sup>Materials Department, University of California, Santa Barbara, CA, CA 93107, United States

<sup>c</sup>Department of Chemistry, Northwestern University, Evanston, IL 60208, United States

<sup>d</sup>Department of Chemistry & Biochemistry,  
University of California, Santa Barbara, CA 93106, United States

Inorganic and hybrid organic–inorganic main-group halides that adopt the perovskite structure combine excellent performance in photovoltaic applications, ease of preparation, and abundant constituent elements, but the origins of their remarkable properties are a matter of debate [1]. Here, we address two unusual aspects of these materials which have significant implications for functionality.

First, X-ray scattering studies reveal local, temperature-activated off-centering of the group 14 cations within their coordination octahedra across the materials class reflecting a preference for lower symmetry coordination than that implied by crystallographic approaches [2,3]. Ab initio calculations, optical measurements, and analogies to existing theory implicate the  $ns^2$  lone pair electrons (and the corresponding second-order Jahn-Teller effect) as the origin of this phenomenon, which we propose leads to enhanced defect screening, reduced thermal conductivity, and unusual temperature-dependence of the electronic bandgap [2]. We further demonstrate tuning of this phenomenon by homovalent chemical substitution on all sites of the perovskite structure [3].

Second, the size, shape, and polarity of the molecular cations are shown to have a profound effect on the temperature evolution of structure and dynamics in the lead iodides [4,5]. In contrast to the well-studied MAPbI<sub>3</sub> (MA = CH<sub>3</sub>NH<sub>3</sub>), FAPbI<sub>3</sub> (FA = HC[NH<sub>2</sub>]<sub>2</sub>) exhibits an unusual reentrant pseudosymmetry on cooling which is reflected in the optical properties, as well as persistent molecular motion below 100 K which indicates a markedly different molecule–cage interaction in the two compounds [5]. Despite markedly different barriers for molecular rotation, solid state nuclear magnetic resonance reveals similar dynamics at ambient temperatures for these high-performance compounds. Lastly, comparisons of the structure evolution of FAPbBr<sub>3</sub> and FASnI<sub>3</sub> from that of FAPbI<sub>3</sub> suggest that the nature of the metal–halogen bond has an inductive effect on the strength of hydrogen bonding to the halogens. This work was supported by the U.S. Department of Energy, Office of Science, Basic Energy Sciences under award number DE-SC-0012541.

### References:

- 1) D. H. Fabini, J. G. Labram, A. J. Lehner, J. S. Bechtel, H. A. Evans, A. Van der Ven, F. Wudl, M. L. Chabinyk, R. Seshadri, *Inorg. Chem.* **56** (2017) 11–25.
- 2) D. H. Fabini, G. Laurita, J. S. Bechtel, C. C. Stoumpos, H. A. Evans, A. G. Kontos, Y. S. Raptis, P. Falaras, A. Van der Ven, M. G. Kanatzidis, R. Seshadri, *J. Am. Chem. Soc.* **138** (2016) 11820–11832.
- 3) G. Laurita, D. H. Fabini, C. C. Stoumpos, M. G. Kanatzidis, R. Seshadri, *Chem. Sci.* **8** (2017) 5628–5635.
- 4) D. H. Fabini, T. Hogan, H. A. Evans, C. C. Stoumpos, M. G. Kanatzidis, R. Seshadri, *J. Phys. Chem. Lett.* **7** (2016) 376–381.
- 5) D. H. Fabini, C. C. Stoumpos, G. Laurita, A. Kaltzoglou, A. G. Kontos, P. Falaras, M. G. Kanatzidis, R. Seshadri, *Angew. Chem. Int. Ed.* **55** (2016) 15392–15396.

# Electronic band structure of $\text{Cu}_2\text{ZnAS}_{4-x}$ and $\text{CuZn}_2\text{AS}_4$ (A = Al, Ga, In) nanocrystals for solar energy conversion applications

Anima Ghosh<sup>a,b</sup> and R. Thangavel<sup>b</sup>

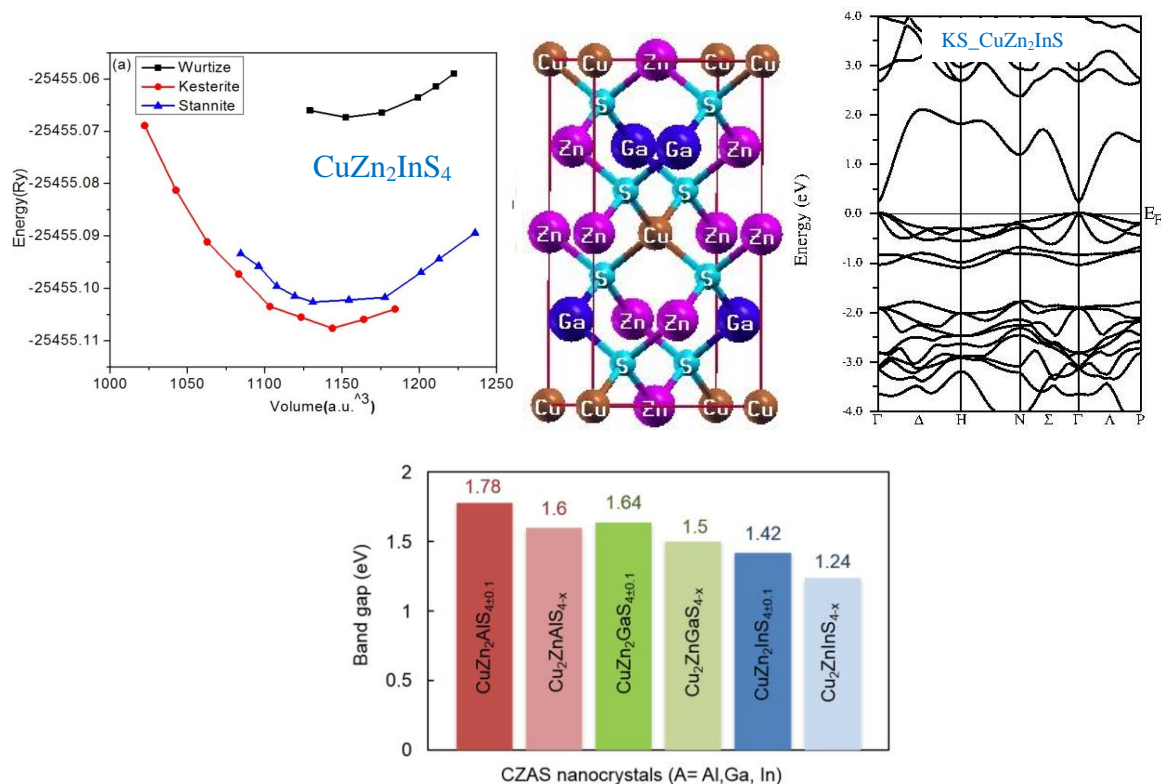
<sup>a</sup>Thin Film Laboratory, Department of Physics, Indian Institute of Technology, New Delhi, India

<sup>b</sup>Solar Energy Research Laboratory, Department of Applied Physics, Indian Institute of Technology (Indian School of Mines), Dhanbad, India

## Abstract:

A new family of quaternary semiconductors  $\text{Cu}_2\text{ZnAS}_{4-x}$  and  $\text{CuZn}_2\text{AS}_4$  (A = Al, Ga, In) has been systematically studied using first-principles calculations as implemented in WIEN2k code. Equilibrium total energy of various possible crystal structures, phase stability, optical transitions and p-d bonding have been analyzed. It can be observed that, the bonding and anti-bonding states overlap more in compounds with heavier III atoms. The optical spectra shift to low energy region from In to Ga. Importantly, these new compositions are direct band gap materials having band gaps between 1.20 eV and 1.72 eV with a high absorption cross-section, as confirmed from experimental absorption measurements and theoretical calculations. Our initial investigations indicate that these materials possess the requisite optical characteristics to be used as cost-effective and nontoxic absorber layers in solar cell applications.

## Highlight few results:



# Searching magnetic phase, electronic structure and thermoelectric properties of $\text{Ti}_2\text{MnAl}$ Heusler material

H. Kara<sup>a,b</sup>, K. Özdoğan<sup>b</sup>

<sup>a</sup>Department of Physics, Necmettin Erbakan University, Konya, 42090, Turkey.

<sup>b</sup>Department of Physics, Yildiz Technical University, İstanbul, 34220, Turkey.

husnukara@konya.edu.tr

Determining correct magnetic phase in magnetic materials is very important to understand real nature of materials. Accurate electronic structure requires correct choice of magnetic phase. To this purpose, we use ab-initio calculations by Wien2k package [1]. PBE-GGA (Perdew-Burkew Ernzerhof 96) exchange correlation potential is used for the total energy calculations [2]. Our total energy calculations show that  $\text{Ti}_2\text{MnAl}$  is stable in antiferromagnetic phase, and then according to antiferromagnetic phase, electronic structure calculations reveal through bandstructure and the density of states that  $\text{Ti}_2\text{MnAl}$  alloy exhibits metallic behaviour by the view of bandstructure and the density of states. After Wien2k, as a sequential code, we also utilize BoltzTraP code [3], which based on Boltzman transport theory, to calculate thermoelectric properties. We present the electronic thermal conductivity, Hall coefficient, Seebeck coefficient, the electrical conductivity, the power factor and the dimensionless figure of merit. Higher dimensionless figure of merit means better conversion ability from heat to electricity in a material [4].

**Keywords:** Magnetic phase, total energy calculations, electronic structure, Heusler material.

## References:

1. P. Blaha, K. Schwarz, G. Madsen, D. Kvasicka, and J. Luitz, WIEN2k, An augmented plane wave plus local orbitals program for calculating crystal properties, T. U. Vienna, Vienna, 2001.
2. Perdew, J. P.; Burke, K.; Ernzerhof, M., Generalized Gradient Approximation Made Simple, Phys. Rev. Lett. 77, 3865-3868, 1996.
3. G. K. H. Madsen and D. J. Singh, Comput. Phys. Commun. 175, 67, 2006.
4. Enrique Macia-Barber, Thermoelectric Materials: Advances and Applications, Pan Stanford, 2015.



# **A DFT based thermoelectric energy research: Co<sub>2</sub>MnSn Heusler alloy as a direct thermal energy conversion material**

**H. Kara<sup>a,b</sup>, K. Özdoğan<sup>b</sup>**

<sup>a</sup>Department of Physics, Necmettin Erbakan University, Konya, 42090, Turkey.

<sup>b</sup>Department of Physics, Yildiz Technical University, İstanbul, 34220, Turkey.

**husnukara@konya.edu.tr**

Thermoelectric conversion have strong points, such as independence of heat amount, no moving parts and power generation by temperature difference, and advantages, such as recovery of dilute waste heat, no maintenance, long lifetime, low cost, less noise and no vibration [1]. For the band structure calculations, the Wien2k program [2], the application of the linearized augmented plane wave (LAPW) method, was used as the DFT code and the BoltzTraP program [3], which calculates semi-classic transport coefficients using Boltzmann transport theory. The material exhibits nearly semiconducting behavior in one spin channel and metallic behavior in the other. Half-metallic Co<sub>2</sub>MnSn ferromagnetic Heusler alloy has an increased energy transfer efficiency with increasing temperature.

**Keywords: Energy research, thermoelectric, DFT, thermal energy conversion material.**

## **References:**

1. Qiang Xu, Tetsuhiko Kobayashi, Advanced Materials for Clean Energy, Crc Press, 2015.
2. P. Blaha, K. Schwarz, G. Madsen, D. Kvasicka, and J. Luitz, WIEN2k, An augmented plane wave plus local orbitals program for calculating crystal properties, T. U. Vienna, Vienna, 2001.
3. G. K. H. Madsen and D. J. Singh, Comput. Phys. Commun. 175, 67, 2006

## First-principles Study of Electronic Properties of Si-doped FeSe<sub>0.9</sub> Alloys

Sandeep Kumar<sup>1,2</sup>, Prabhakar P. Singh<sup>1</sup> and Dan Thomas Major<sup>2</sup>

<sup>1</sup>*Department of Physics, Indian Institute of Technology Bombay, Powai, Mumbai 400076, India*

<sup>2</sup>*Department of Chemistry, Bar-Ilan University, Ramat Gan 52900, Israel*

*Email: sandeepk.phy@gmail.com*

Alloying and doping have always been an effective way of improving the properties of materials, be it electronic, magnetic or superconducting. In this, we performed first-principles calculations of electronic and superconducting properties of FeSe<sub>0.9-x</sub>Si<sub>x</sub> ( $x = 0.0, 0.05$ ) alloys using the Green's function Korringa-Kohn-Rostoker Atomic Sphere Approximation within the coherent potential approximation (KKR-ASA-CPA), based on density functional theory [1-4]. The CPA approach is used to handle the disorder in the systems. Our calculations show that these alloys are nonmagnetic in nature. We found that the substitution of Si at Se sites into FeSe<sub>0.9</sub> yielded subtle changes in the electronic structure with respect to the parent FeSe. The results have been analysed in terms of changes in the density of states (DOS), band structures, Fermi surfaces (FS) and the superconducting transition temperature ( $T_c$ ) of FeSe<sub>0.9</sub> and FeSe<sub>0.85</sub>Si<sub>0.05</sub> alloys. In particular, we find that the Si-doped FeSe<sub>0.9</sub> exhibits the same topology of the FS as that of FeSe, differing only in subtle FS nesting features. Our calculations show that the calculated  $T_c$  for these alloys are close to experimental values.

**Keywords:** Electronic Structure, KKR-ASA-CPA, DFT, Disordered, Alloys

### References:

1. Kamihara Y et al., J. Am. Chem. Soc. **130**, 3296 (2008).
2. Hsu FC et al., Proc. Natl. Acad. Sci. U.S.A **105**, 14262 (2008).
3. J.S. Faulkner. Prog. Mat. Sci., 27:1, 1982.
4. Sudesh et al. Physica C: Superconductivity 485 137 (2013).

# MAGNETIC ANISOTROPY AND SPECTROSCOPIC PROPERTIES OF $\text{SeCuO}_3$

William Lafargue-Dit-Hauret<sup>1</sup>, Vinko Šurija<sup>2</sup>, Tonči Cvitanić<sup>3</sup>, Mihael Grbić<sup>3</sup>, Mirta Herak<sup>2</sup>,  
Xavier Rocquefelte<sup>1</sup>

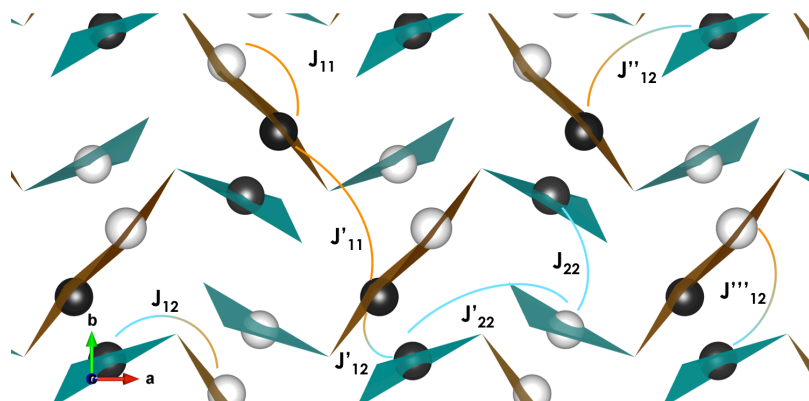
<sup>1</sup>*Institut des Sciences Chimiques de Rennes, UMR CNRS 6226, Université de Rennes 1, 263  
Avenue du Général Leclerc, 35042 Rennes, France*

<sup>2</sup>*Institute of physics, Bijenička 46, HR-10000 Zagreb, Croatia*

<sup>3</sup>*Department of Physics, Faculty of Science, University of Zagreb, Bijenička 32, HR-10000  
Zagreb, Croatia*

Presenting author: [william.lafargue-dit-hauret@univ-rennes1.fr](mailto:william.lafargue-dit-hauret@univ-rennes1.fr)

Low-dimensional spin structures are of fundamental interest to investigate magnetic anisotropy and unusual local magnetic properties. In this study, the  $\text{SeCuO}_3$  tetramer-like spin system was studied combining experimental and theoretical DFT calculations. Magnetic susceptibility, ESR spectroscopy and NQR measurements have evidenced that this compound exhibits an highly anisotropic antiferromagnetic behavior [1-3]. More recently, we have carried out neutron scattering and NQR/NMR measurements. To explain these new data, collinear and non-collinear calculations were performed using the VASP code. In addition, Electric Field Gradient and Hyperfine Field quantities have been estimated using the WIEN2k code and are compared to our NQR/NMR data.



*Magnetic exchange coupling considered theoretically between Cu atoms.*

- [1] I. Živković, D. M. Djokić, M. Herak, D. Pajić, K. Prša, P. Pattison, D. Dominko, Z. Michković, D. Cinčić, L. Forró, H. Berger, and H. M. Rønnow. Phys. Rev. B 86 (2012) 054405
- [2] M. Herak, A. Grubišić Čabo, D. Žilić, B. Rakvin, K. Salamon, O. Milat, and H. Berger. Phys. Rev. B 89 (2014) 184411
- [3] S. Lee, W.-J. Lee, J. van Tol, P. L. Kuhns, A. P. Reyes, H. Berger, and K.-Y. Choi. Phys. Rev. B 95 (2017) 054405

# Experimental and Theoretical Investigation of a Photovoltaic glass-ceramic material based on the heterojunction $\text{Sb}_2\text{Se}_3$ - $\text{GeSe}_2$ - $\text{CuI}$

Alicia LECOMTE<sup>1</sup>, Xavier ROCQUEFELTE<sup>1</sup>, Camille LATOUCHE<sup>2</sup>,  
Laurent CALVEZ<sup>1</sup>, XiangHua ZHANG<sup>1</sup>

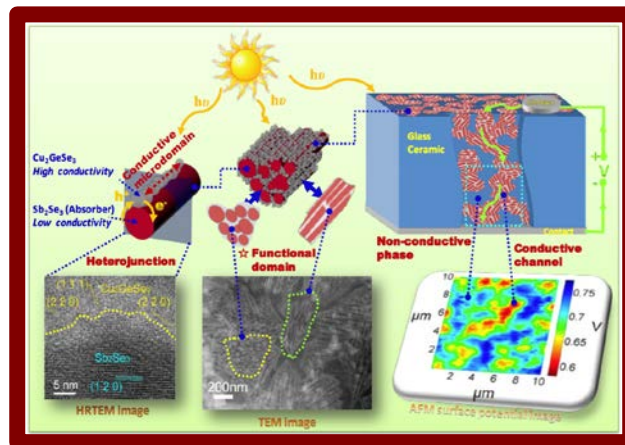
<sup>1</sup> Institut des Sciences Chimiques de Rennes, UMR 6226, Université de Rennes 1,  
263 Avenue du Général Leclerc, 35042 Rennes, France

<sup>2</sup> Institut des Matériaux Jean Rouxel (IMN), UMR 6502, Université de Nantes, CNRS, 2 rue  
de la Houssinière, BP 32229, 44322 Nantes cedex 3, France

e-mail : alicia.lecomte@univ-rennes1.fr

Photovoltaic materials are nowadays essential in our daily life, but many efforts are still needed to improve their performances and reduce their cost. Here, we have considered a glass-ceramic compound, which has been discovered in our lab [1]. It exhibits a photoelectric current arising from a p-n heterojunction. Here we show our preliminary experimental and theoretical results, which aimed to characterize properly the chemical nature of material compound. We will discuss about the origin of the n-type conductivity of  $\text{Sb}_2\text{Se}_3$ . Finally, PyDEF software [3] is used to define the charge state of the defects responsible of the p-n junction.

The first idea about the possible mechanism of charge photogeneration, separation and transport can be proposed in the figure.



[1] L. Calvez, H.L. Ma, J. Lucas, X.H. Zhang. Journal of Non-Crystalline Solids 354 (2008) 1123–1127

[2] X.H. Zhang, Y. Xu, Q. Shen, B. Fan. Journal of Materials Chemistry A, 2014, 2, 17099–17106

[3] E. Péan, J. Vidal, S. Jobic C. Latouche. Chemical Physics Letters. 671 (2017) 124-130



# Electronic and magnetism properties of vacancy-defected and adsorption on MoO<sub>3</sub> (010) Surface: a first-principles study

Masoud Mansouri<sup>1,2\*</sup>, Tahereh Mahmoodi<sup>1</sup>, Raheleh Kimia<sup>1</sup>

<sup>1</sup>Department of physics, Mashhad Branch, Islamic Azad University, Mashhad, Iran

<sup>2</sup>Computational Science Research Center, Applied Biology Institute, Mashhad Branch, Islamic Azad University, Mashhad, Iran.

**Abstract.** In this work, a systematic DFT calculation was carried out to investigate the effects of various kinds of dopants on the electronic structure of MoO<sub>3</sub> (010) Surface. The possibility to obtain magnetic phase from native defects in orthorhombic MoO<sub>3</sub> is investigated. We find that both Mo and O vacancies can induce a magnetic phase of  $\sim 2 \mu_B$  with a local magnetic moment, whereas corresponding Mo vacancies ( $V_{Mo}$ ) provides the transition of the insulating molybdenum trioxide into a metallic-like phase and changes the electronic transport. Next, we present results on the influence of the common gas molecules on the electrical resistivity. The most stable configurations, magnetism, adsorption energies and electronic properties are thoroughly discussed. Due to the calculated adsorption energies, we find that MoO<sub>3</sub> bilayers exhibit suitable parameters for serving as a gas sensor. Among the possible elemental doping, we find that Lithium adsorption shifts the Fermi level into the MoO<sub>3</sub> conduction band and makes the n-type semiconducting.

**Keywords:** Molybdenum trioxide, Surface, Vacancy, Dopant, Gas adsorption, DFT

**Introduction-** In recent decades, transition metal oxides with layered crystalline structures are studied extensively for their significant physical, chemical, multifaceted structural and functional diversity [1, 2]. the intrinsic properties of a large diversity of Mo-containing systems have been investigated in detail, in particular to elucidate relationships among the electronic structure of these systems and their catalytic behaviors [3]. Indeed, Materials who are composed of atoms which are covalently bonded in two-dimensional (2D) planar spaces are considered quasi 2D materials [4]. One of the most important is molybdenum-trioxide (Molybdite). It is attractive for its photochromic, thermochromic properties and it is a widely used catalytic, gas sensing precursor, electrochromic as optical devices, production and promotion of field-effect transistors and micro batteries as electronic tools [5-8].

According to the experimental studies, the most stable thermodynamically phase crystallizes in the simple orthorhombic crystal structure (space group *Pbnm*) with lattice constants  $a = 3.962 \text{ \AA}$ ,  $b = 13.855 \text{ \AA}$  and  $c = 3.697 \text{ \AA}$  [9, 10]. This structure is made by a series of bilayers which are oriented stand-up to the (010) Y-axis. These bilayers, coupled to each other by weak van der Waals' interaction, while internal bonds are formed by covalent and ionic bonds. The three oxygen atoms are grouped into three types, i.e. terminal oxygen ( $O_1$ ), asymmetric bridging oxygen ( $O_2$ ), and symmetric bridging oxygen ( $O_3$ ) [11, 12].

The bulk of MoO<sub>3</sub>, in its intrinsic form is an indirect wide band gap material ( $\sim 2.8 \text{ eV}$ ), so due to the low carrier concentration, the pure case is not suitable for electronic tools [13-15]. particularly, band gap engineering is one of the best approaches via impurity dopant for tuning gap states between the valence band (VB) and conduction band (CB) [16, 17]. The most common procedure is adopted by Hydrogen and alkali metals. Basically, band filling is used to set the optical and electronic specifications. Indeed, the defected states by vacancies may also diminish the band gap.

The aim of this work is to simulate MoO<sub>3</sub> (010) surface with most stable structure and investigate its electronic structure. Next we consider defect states and various MoO<sub>3</sub> dopant concentrations via the cases of adsorption of gas molecule on the topmost O atom ( $O_3$ ) as potential applications in catalysis, gas sensing. Finally, we study different intercalation of Li-ion by substitutional and adsorbed configuration. The mechanism of Lithium intercalation is the basis for material's application as the electrode in the rechargeable batteries[18].

## Reference

- [1] H.H. Kung, *Transition metal oxides: surface chemistry and catalysis*, (Elsevier, 1989).
- [2] P.A. Cox, *Transition metal oxides: an introduction to their electronic structure and properties*, (Oxford university press, 2010).
- [3] F. Solymosi, J. Cserenyi, A. Szöke, T. Bansagi, A. Oszko, *Journal of Catalysis* **165**, 150 (1997).
- [4] P.J. Zapf, R.L. LaDuca, R.S. Rarig, K.M. Johnson, J. Zubieta, *Inorganic Chemistry* **37**, 3411 (1998).
- [5] K. Galatsis, Y. Li, W. Wlodarski, E. Comini, G. Sberveglieri, C. Cantalini, S. Santucci, M. Passacantando, *Sensors and Actuators B: Chemical* **83**, 276 (2002).
- [6] B.W. Faughnan, R.S. Crandall, *Applied Physics Letters* **31**, 834 (1977).
- [7] L. Zhou, L. Yang, P. Yuan, J. Zou, Y. Wu, C. Yu, *The Journal of Physical Chemistry C* **114**, 21868 (2010).
- [8] M. Quevedo-Lopez, R. Reidy, R. Orozco-Teran, O. Mendoza-Gonzalez, R. Ramirez-Bon, *Journal of Materials Science: Materials in Electronics* **11**, 151 (2000).
- [9] L. Kihlberg, *Arkiv for Kemi* **21**, 357 (1963).
- [10] G. Andersson, A. Magneli, *Acta Chem. Scand* **4**, 793 (1950).
- [11] D.O. Scanlon, G.W. Watson, D. Payne, G. Atkinson, R. Egdell, D. Law, *The Journal of Physical Chemistry C* **114**, 4636 (2010).
- [12] P.-R. Huang, Y. He, C. Cao, Z.-H. Lu, *Scientific reports* **4**, (2014).
- [13] A. Bouzidi, N. Benramdane, H. Tabet-Derraz, C. Mathieu, B. Khelifa, R. Desfeux, *Materials Science and Engineering: B* **97**, 5 (2003).
- [14] J.Z. Ou, J.L. Campbell, D. Yao, W. Wlodarski, K. Kalantar-Zadeh, *The Journal of Physical Chemistry C* **115**, 10757 (2011).
- [15] H. Martínez, J. Torres, L. López-Carreño, M. Rodríguez-García, *Journal of superconductivity and novel magnetism* **26**, 2485 (2013).
- [16] T.J. Drummond, P.L. Gourley, T.E. Zipperian, *IEEE Spectrum* **25**, 33 (1988).
- [17] F. Capasso, *Science* **235**, 172 (1987).
- [18] J.-M. Tarascon, M. Armand, *Nature* **414**, 359 (2001).

# The Magnetic Properties Investigation of Nickel and Cobalt Oxyborate Compounds with a Kotoite Structure

Nazarenko I.I.<sup>a</sup>, Sofronova S.N.<sup>a</sup>, Moshkina E.M.<sup>a,b</sup>

<sup>a</sup> L.V. Kirensky Institute of Physics SB RAS, 660036 Krasnoyarsk, Russia

<sup>b</sup> Siberian State Aerospace University named after Academician M.F. Reshetnev, 660037 Krasnoyarsk, Russia

Close attention was focused on the compounds with geometric magnetic frustrations, since these materials can have interesting magnetic properties and magnetic states (spin glass, spin liquid and spin ice). A characteristic feature of these compounds is the presence of triangular or tetrahedral groups in the structure, which form chains and bands (Figure1). Oxyborates  $M_3B_2O_6$  ( $M = \text{Co}, \text{Ni}$  or  $\text{Mn}$ ) with the structure of the kotoite [1] contain structural elements that are necessary for the emergence of interesting magnetic features: in their structure, there are triangular groups and all metal ions are localized inside the oxygen octahedra.

In this study, we performed density functional calculations [2] for studying the crystal, electron, and magnetic structure of  $\text{Ni}_3\text{B}_2\text{O}_6$ . The exchange and correlation functional was processed using the local spin density approximation (LSDA) and LSDA + U, and the approximation of the generalized gradient Perdew-Burke Ernzerhof (GGA-PBE) and GGA-PBE + U, due to the strong correlations in our material. In addition, we would like to present an extensive analysis of the electronic structure, charge density and exchange interactions.

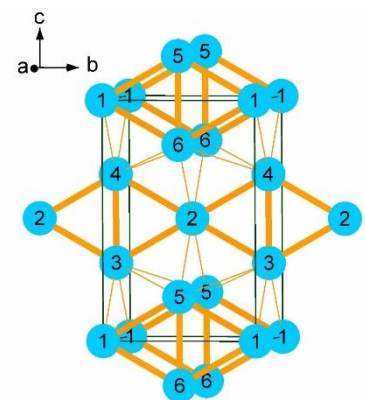


Figure1. The unit cell of the kotoite structure. Bold lines show triangular groups in the plane  $bc$ . Oxygen and boron ions are omitted. Ions 1, 2 refer to the crystallographic position  $2a$ , ions 3-6 to position  $4f$ .

## References

- [1] R. Newnham, R. Santoro, P. Seal and G. Stallings, "Antiferromagnetism in  $\text{Mn}_3\text{B}_2\text{O}_6$ ,  $\text{Co}_3\text{B}_2\text{O}_6$ , and  $\text{Ni}_3\text{B}_2\text{O}_6$ ," *Physica Status Solidi (b)*, vol. 16, no. 1, pp. K17-K19, 1966.
- [2] W. Kohn and L. J. Sham, "Self-Consistent Equations Including Exchange and Correlation Effects," *Physical Review*, vol. 140, no. 4A, p. A1133, 15 November 1965.

# Mn-oxalates - experimental and theoretical approach

*M. Nedyalkova*<sup>1</sup> *H. Alexandrov*<sup>2</sup> *B. Donkova*<sup>1</sup> *I. Koleva*<sup>2</sup>

<sup>1</sup> Sofia University Faculty of Chemistry and Pharmacy, Department of Inorganic Chemistry 1164 Sofia, 1 James Bourchier Blvd.

<sup>2</sup> Sofia University Faculty of Chemistry and Pharmacy, Department of Organic Chemistry 1164 Sofia, 1 James Bourchier Blvd.

In a system containing  $\text{Mn}^{2+}$ –  $\text{C}_2\text{O}_4^{2-}$ –  $\text{H}_2\text{O}$  three crystal forms could be obtained depending on the synthesis conditions – monoclinic  $\alpha$ - $\text{MnC}_2\text{O}_4 \cdot 2\text{H}_2\text{O}$  (SG C2/c), orthorhombic  $\gamma$ -  $\text{MnC}_2\text{O}_4 \cdot 2\text{H}_2\text{O}$  (P212121) and orthorhombic trihydrate  $\text{MnC}_2\text{O}_4 \cdot 3\text{H}_2\text{O}$  (Pcca). For the latter the formula  $\{[\text{Mn}(\mu\text{-C}_2\text{O}_4)(\text{H}_2\text{O})_2] \cdot \text{H}_2\text{O}\}_n$  is recommended. All of them are one-dimensional structures with molecular-based magnetism where the oxalate mediates magnetic exchanges by bridging paramagnetic  $\text{Mn}^{2+}$  centers. However, the difference in the crystal lattice suggests the different strength of magnetic *intra- and inter-chain* interaction. It is well known the antiferromagnetic behaviour of the three forms. To explain the magnetic properties and to estimate the magnetic coupling constant  $J$  of these periodic systems the hybrid density functional theory (DFT) was applied because it accounts the electronic correlation effects which are not involved in Anderson model, Heisenberg model or broken symmetry (BS) approach. The simulated XRD and NMR spectra were compared with experimental ones.



# Optimised structural models of solid solutions for tensorial properties

Dominik Nöger, David Holec  
Montanuniversität Leoben,  
Austria

## ABSTRACT

**S**pecial **Q**uasirandom **S**tructures (SQS) proved successful for modelling random disordered alloys in conjunction with the density functional theory. This approach uses a single disordered supercell to mimic a real alloy, and to model those properties which depend on the local atomic configurations. However, the available computing resources are steadily growing, which leads to bigger supercells, and consequently to exponentially growing number of possibilities how to arrange atoms in a supercell. An efficient implementation is presented for optimising WARREN-COWLEY short range order parameters, describing the local disorder, of given supercells. As optimisation methods *Monte-Carlo* for big, and a *systematic* approach for small supercells were implemented, enabling to check  $\approx 10^{10}$  to  $10^{11}$  atomic configurations even on commodity hardware, and cycle times of  $< 5 \cdot 10^{-7}$  seconds per configuration when parallelization is enabled on bigger machines. Furthermore elastic stiffness tensors were calculated for supercells which are equal in terms of the SQS methodology to show up the limits of accuracy of the approach when it comes to tensorial properties. The last part deals with the comparison of elastic properties of **D**irectional **O**ptimized **S**pecial **Q**uasirandom **S**tructures (DOSQS) and regular SQS cells for different crystal systems (A4 *diamond*  $\text{Si}_{0.5}\text{Ge}_{0.5}$ , A1 *fcc*  $\text{Ag}_{0.5}\text{Au}_{0.5}$  and A2 *bcc*  $\text{W}_{0.5}\text{Mo}_{0.5}$ ).

# A first principle calculation of half metallic ferromagnetism in transition metal doped BeS

Hardev Singh<sup>1,†</sup>, and Manish K. Kashyap<sup>2</sup>

<sup>1</sup>Department of Physics, GJUS&T Hisar-125001 (Haryana) India

<sup>2</sup>Department of Physics, Kurukshetra University, Kurukshetra-136119 (Haryana), India

<sup>†</sup>E-mail:hardevdft@gmail.com

Diluted magnetic semiconductors (DMSs) are the imperative spintronic materials because these materials show the half metallic ferromagnetism (HMF) and high spin polarization at fermi level ( $E_F$ ) on suitable doping with appropriate atoms. There exists plethora of experimental [1,2] and theoretical [3,4] studies which focus on crucial properties of DMS compounds. From last few years, transition metal (TM) doped DMS compounds have attracted much attention of the researchers due to the possibility of improved HMF. In order to support the experimental observations, we planned to remain focused on the first principle calculation of electronic and magnetic properties of Ti and V-doped BeS DMS compound.

The ground state calculations of  $Be_{1-x}TM_xS$  (TM=Ti and V) compound at doping concentration,  $x = 0.03$ , have been performed using FPLAPW method based on density functional theory (DFT) [5] as implemented in WIEN2k code [6]. The exchange and correlation (XC) potentials were constructed using GGA within the parameterization of Perdew-Burke-Ernzerhof (PBE) [7]. The present calculations were based on the supercell approach where one Be atom at (0,0,0) in the supercell of BeS was replaced by transition metal (TM) atom. In order to generate 3.125% Ti and V-doping in BeS, a cubic supercell, (2×2×2) was constructed.

We have found that the ground state properties of bulk BeS compound get modified significantly due to the substitution of dopant at the cation (Be) site. The new states are produced at  $E_F$  which accounts for the magnetism on the doping. We have realized that the ferromagnetism in BeS remarkably depends on the TMs. The emergence of half metallic ferromagnetism in Ti, V-doped BeS compound can be explained by Zener's double exchange mechanism for ferromagnetism as in other DMS compounds. The HMF characteristics of Ti, V-doped BeS compound makes it an ideal material for spintronic devices.

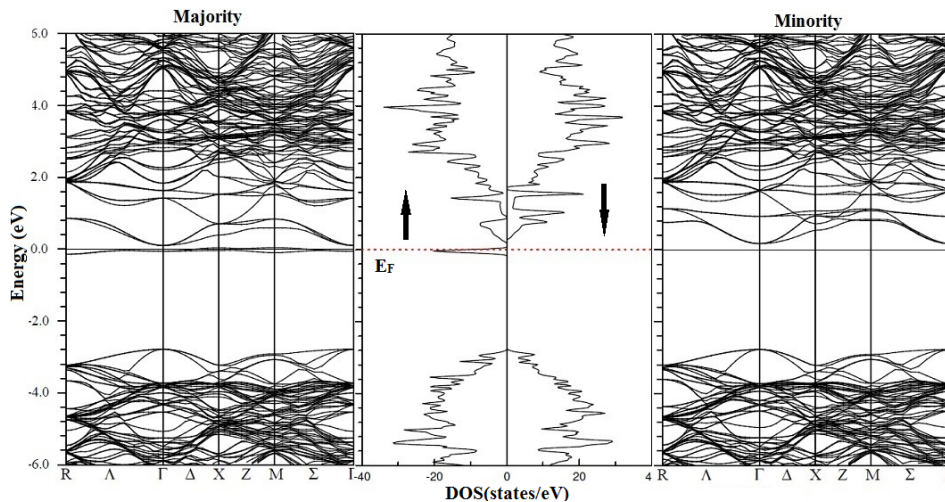


Fig. 1 Spin resolved band structure and total DOS of  $\text{Be}_{1-x}\text{Ti}_x\text{S}$  ( $x = 0.03$ ). The horizontal line at  $E = 0$  eV

## References

- [1] E. Abe, K. Sato, F. Matsukura, J.H. Zhao, Y. Ohno, H. Ohno, *J. Supercond.: Incorpor. Novel Magn.* 17 (2004) 349.
- [2] K.Y. Ko, M.G. Blamire, *Appl. Phys. Lett.* 88 (2006) 172101.
- [3] H.S. Saini, M. Singh, A.H. Reshak, M.K. Kashyap, *J. Alloy Comps.* 536 (2012) 214.
- [4] S. Nazir, N. Ikram, S.A. Siddiqi, Y. Saeed, A. Shaukat, A.H. Reshak, *Cur. Opin. Solid State Mater. Sci.* 14 (2010) 6.
- [5] P. Hohenberg, W. Kohn, *Phys. Rev.* **136**, B864 (1964).
- [6] P. Blaha, K. Schwarz, G.K.H. Madsen, D. Kvasnicka, J. Luitz: WIEN2k, An augmented plane wave + Local Orbitals Program for calculating Crystal Properties, Techn. Universitat Wien, Wien, Austria, 2001, ISBN 3-9501031-1-2.
- [7] P. Perdew, K. Burke and M Ernzerhof, *Phys. Rev. Lett.* 77, 3865 (1996)

## **Spin gapless character of Ti<sub>2</sub>MnAl inverse Heusler alloy under uniform and tetragonal strain**

Mukhtiyar Singh<sup>a,\*</sup>, Manoj K. Sharma<sup>b</sup>, Hardev S. Saini<sup>c</sup>, Manish K. Kashyap<sup>d</sup>

<sup>a</sup>*Department of Physics, Delhi Technological University, Delhi-110042 (Delhi), India*

<sup>b</sup>*Kendriya Vidyalaya No. 1, Kanchrapara-743193 (West Bengal), India*

<sup>c</sup>*Department of Physics, Guru Jambheshwar University of Science & Technology-125001(Haryana), India*

<sup>d</sup>*Department of Physics, Kurukshetra University, Kurukshetra-136119 (Haryana), India*

\*Email: [msphysik09@gmail.com](mailto:msphysik09@gmail.com), [mukhtiyarsingh@dtu.ac.in](mailto:mukhtiyarsingh@dtu.ac.in)

In the present study, inverse Heusler alloy based spin-gapless semiconductor (SGS), Ti<sub>2</sub>MnAl is investigated using full potential linearized augmented plane wave (FP-LAPW) method implemented in WIEN2k crystal programme. Our investigation reveals that this alloy behaves as SGS, with zero total magnetic moment, for equilibrium lattice constant (6.23 Å). Further, it keeps its spin gapless state within -15% to 10% uniform strain. On the other hand for -5% of tetragonal strain, the system behaves as SGS whereas the positive 5% tetragonal strain completely destroys the spin-gapless character of Ti<sub>2</sub>MnAl Heusler alloy. The band gap in up spin channel for Ti<sub>2</sub>MnAl is 0.55 eV and 0 eV for spin down channel for equilibrium lattice constant. It varies up to a maximum value of 0.31 eV and 0.36 eV for positive and negative uniform strain, respectively. The value of this gap for -5% and 5% of tetragonal strain is 0.51 eV and 0.46 eV, respectively. Our calculations provide an exhaustive data to be compared with future experiments and advocate the future applications of this alloy in spintronic applications.



# Planar versus three-dimensional growth of metal nanostructures at 2D heterostructures

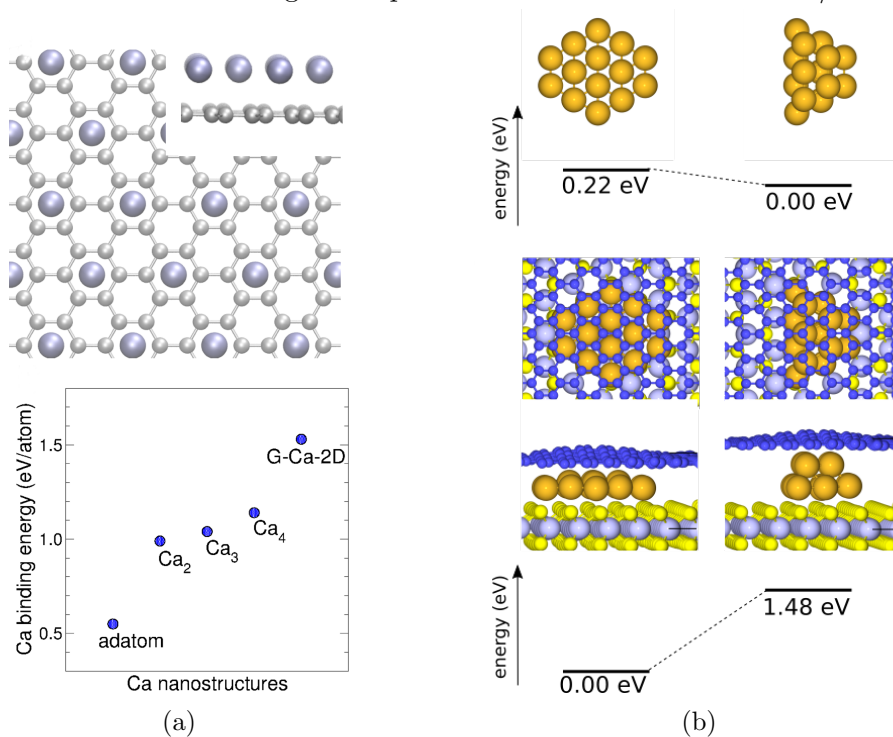
S. Stavrić<sup>1</sup>, M. Belić<sup>2</sup>, Ž. Šljivančanin<sup>1,2</sup>

<sup>1</sup> Vinča Institute of Nuclear Sciences, 11000 Belgrade, Serbia

<sup>2</sup> Texas AM University at Qatar, Education City, Doha, Qatar  
[stavric@vinca.rs](mailto:stavric@vinca.rs)

Employing DFT we studied microscopic mechanisms governing initial stages of growth of few selected metals on graphene (G), as well as influence of MoS<sub>2</sub> on this behavior when metals are used as intercalators in G/MoS<sub>2</sub> heterostructures. Tendency towards planar (2D) or three-dimensional (3D) growth is rationalized based on atomic-scale description of the interaction between adsorbates. Li atoms, featuring a long-ranged electrostatic repulsion, are individually dispersed across the G surface, in a sharp contrast with atoms of transition metal Ti which gather into densely-packed 3D clusters due to a strong short-ranged metal-metal attraction. Modest attractive interaction between Ca adatoms on G enable formation of stable monoatomic films with the local coverage of 1/6 monolayer (ML). Though Au clearly arrange into 3D structures on pristine G, when used as intercalator in G/MoS<sub>2</sub> it shows strong preference for 2D growth, forming G/Au-ML/MoS<sub>2</sub> heterostructure with weakly interacting constituents where Au ML closely resemble electronic properties of the hypothetical free-standing hexagonal Au monolayer.

Figure 1: a) 2D nanostructure of Ca on graphene (G-Ca-2D) and comparison between binding energies of different Ca nanostructures on graphene. b) Energy difference between small 2D and 3D Au clusters in gaseous phase and when intercalated in G/MoS<sub>2</sub>.



## References

- [1] Planar versus three-dimensional growth of metal nanostructures at graphene, S. Stavrić, M. Belić, Ž. Šljivančanin, *Carbon* 96 (2016) 216-222
- [2] Graphene/MoS<sub>2</sub> Heterostructures as Templates for Growing Two-Dimensional Metals: Predictions from Ab-initio Calculations, Ž. Šljivančanin, M. Belić, to be published in *Phys. Rev. Mater.*

# Theoretical study of structural, electronic and magnetic properties in $Mn_2RuSn$ and $Mn_2RuGe$ Heusler alloys: Cu<sub>2</sub>MnAl type and Hg<sub>2</sub>CuTi type.

Bouchra TAYCHOUR<sup>1</sup>, Lalla Btissam DRISSI<sup>1,2</sup>

<sup>1</sup> LPHE, Modeling and Simulations, Faculty of Science, Mohammed V University, Rabat, Morocco

<sup>2</sup> CPM, center of physics and mathematics, Faculty of sciences, Mohammed V University, Rabat, Morocco

Heusler systems with a stoichiometric chemical formula of  $X_2YZ$  or  $Y_2XZ$  [1] (X and Y are transition metals and Z main group elements) have drawn considerable attention [2]. The electronic structure and the magnetic properties in  $Mn_2RuGe$  and  $Mn_2RuSn$  are calculated from first principles, the calculations are based on the local density approximation, and we use the Korringa-Kohn-Rostoker coherent potential approximation (KKR-CPA) method for simulating substitutional and magnetic disorder. The defect calculations are performed by increasing degree of Mn(A)–Ru(C) atomic disorder to determine which type of structure adopts these Heusler alloys. Based on the calculated results, the exchange interaction was determined.

[1] H.C. Kandpal, G.H. Fecher, C. Felser, J. Phys. D: Appl. Phys., 1507, 40 (2007).

[2] T. Graf, C. Felser, S.S.P. Parkin, Prog. Solid State Chem. 39, 1 (2011).

E-mail for corresponding author: [taychour.bouchra@gmail.com](mailto:taychour.bouchra@gmail.com)

# EFG study of orbital melting and Jahn-Teller distortions in LaMnO<sub>3</sub> Manganite

R. Teixeira<sup>1\*</sup>, G.N.P. Oliveira<sup>1</sup>, M. B. Barbosa<sup>1</sup>, J. N. Gonçalves<sup>2</sup>, J. Schell<sup>3,4</sup>, T. M. Mendonça<sup>4</sup>, J.G. Correia<sup>5</sup>,  
A.M.L. Lopes<sup>1</sup> and J. P. Araujo<sup>1</sup>

<sup>1</sup> IFIMUP and IN-Institute of Nanoscience and Nanotechnology, University of Porto

<sup>2</sup> CICECO, Universidade de Aveiro

<sup>3</sup> University of Saabruken, Germany

<sup>4</sup> CERN, CH-1211 Geneva 23, Switzerland

<sup>5</sup> Centro de Ciências e Tecnologias Nucleares, Instituto Superior Técnico, University of Lisbon

\*e-mail: ricardo.c.teixeira@ist.utl.com

In the last years, a deep focus has been devoted to manganites and their exquisite properties triggered by the interplay of spin, orbital, charge and structural degrees of freedom, driven by both fundamental interest and possible applications on colossal magnetoresistance, magnetocaloric and multiferroic properties [1].

In addition, low-cost AMnO<sub>3</sub>, as well as its doped counterparts, have shown promising results for catalyst solutions [2]. In these systems orbital occupancy of the metal ion, orbital order and the Jahn-Teller effect play a critical role on the material's macroscopic properties.

In this work, Ab initio density functional theory calculations were carried out for the prototype LaMnO<sub>3</sub> under two different magnetic configurations. Different values of the on-site Coulomb parameters were used. Direct comparison with the experimental EFG temperature evolution obtained by Perturbed Angular Correlation Technique (PAC) at the La site in LaMnO<sub>3</sub> was done by performing calculations with diluted Cd supercells for two temperatures across the Jahn-Teller and orbital order/disorder transition. Experimentally an unexpected drastic change in the EFG parameters was observed at temperatures much below the Jahn-Teller transition, pointing to a new characteristic temperature in this system. This result gives further proof of the recently reported [3,4] partial melting of the system's orbital order occurring in this system at temperatures much below the order/disorder transition.

1. Electric Field Control of Terahertz Polarization in a Multiferroic Manganite with Electromagnons, A. Shuvaev, V. Dziom, Anna Pimenov et al., Phys. Rev. Lett. 111, 227201 (2013)
2. Design principles for oxygen-reduction activity on perovskite oxide catalysts for fuel cells and metal-air batteries, J. Suntivich, H. Gasteiger, N. Yabuuchi et al., Nature Chemistry 3, 546–550 (2011)
3. Melting of the orbital order in LaMnO<sub>3</sub> probed by NMR, A. Trokiner, S. Verkhovskii, A. Gerashenko et al, Phys. Rev. B 87, 125142 (2013)
4. ESR evidence for partial melting of the orbital order in LaMnO<sub>3</sub> below the Jahn-Teller transition, S. Schaile, H.-A. Krug von Nidda, J. Deisenhofer et al, Phys. Rev. B 90, 054424 (2014)

# Suppression of magnetism under pressure in FeS: A DFT+DMFT study

A.V. Ushakov, A. O. Shorikov, V. I. Anisimov, N. V. Baranov, and S. V. Streltsov

M.N. Mikhhev Institute of Metal Physics of Ural Branch of Russian Academy of Sciences, 620137 Ekaterinburg, Russia

We investigate the evolution of the magnetic properties in FeS under pressure and show that these cannot be explained solely in terms of the spin-state transition from a high to low spin state due to an increase of the crystal field. Using a combination of density functional theory and dynamical mean-field theory (DFT+DMFT), our calculations show that at normal conditions the  $\text{Fe}^{2+}$  ions are in the  $3d^6$  high-spin ( $S=2$ ) state, with some admixture of a  $3d^7\bar{L}$  ( $S=3/2$ ) configuration, where  $\bar{L}$  stands for the ligand hole. Suppressing the magnetic moment by uniform compression is related to a substantial increase in electron delocalization and occupation of several lower spin configurations. The electronic configuration of FeS ions cannot be characterized by a single ionic state, but only by a mixture of the  $3d^7\bar{L}$ ,  $3d^8\bar{L}^2$  and  $3d^9\bar{L}^3$  configurations at pressures  $\sim 7.5$  GPa. The local spin-spin correlation function shows well-defined local magnetic moment, corresponding to a large lifetime in the high state at normal conditions. Under pressure FeS demonstrates a transition to a mixed state with small lifetimes in each of the spin configurations.

# Verification of ab-initio mixing enthalpy using thermodynamic simulation of phase equilibrium and the temperature dependences of the heat capacity of the bcc ferro- and paramagnetic Fe-Cr alloys

Alexander Udovsky<sup>1,2</sup>, Dmitry Vasilyev<sup>1</sup>

<sup>1</sup>Baikov Institute of Metallurgy and Material Sciences of RAS

<sup>2</sup>National Research Nuclear University (MEPhI), Moscow, Russia

For understanding the diffusion processes taking place in materials working under harsh conditions, it is expedient to conduct the computer simulations. In its own turn, suitable interatomic potentials are needed to simulate the kinetic processes. Mixing energy is the most important parameter for the precipitation kinetics as it determines the solubility limit of the system [1]. Interatomic potential parameters, total and mixing energies, activation energies, vacancy migration energies and other parameters, which are necessary for conducting the kinetic simulations, are frequently calculated by fitting to results of ab initio calculated usually at 0K. But since ab initio calculations do possess limitations and uncertainties (as other computational methods), the results obtained from those calculations need to be checked and verified by comparing them to experiments or thermodynamics data, in particular taking the effect of temperature on the energy of mixing into account.

The proposed approach [2] allowed performing verification of ab-initio calculation results obtained by different authors for Fe-Cr mixing enthalpy at 0K, was used to assess the chemical part of the mixing enthalpy of Fe-Cr alloys. Analysis of calculated phase diagram fragments and the temperature dependences of heat capacities for two alloy compositions, and their comparison with experimental data (FIG. 1) has allowed us to estimate the degree of reliability of various approximations used in ab-initio calculations, and thereby realize their verification for further practical use.

References: [1] E. Vincent, C.S. Becquart, C. Pareige, P. Pareige, C. Domain. *JNM* **373** (2008) 387-401; [2] A. L. Udovsky and D. A. Vasilyev, *IOP Conf. Series: Materials Science and Engineering* **130** (2016) 012065, <http://iopscience.iop.org/article/10.1088/1757-899X/130/1/012065/meta> .

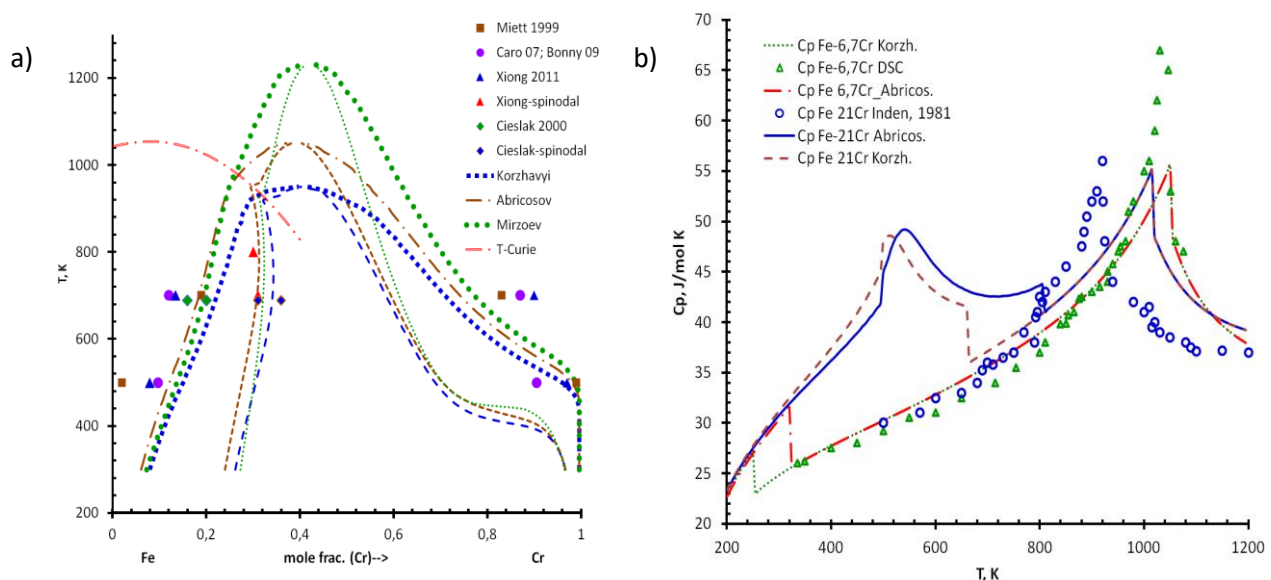


FIG. 1: The calculated miscibility gaps and spinodal curves of bcc Fe-Cr alloys (a), the temperature dependences of isobaric heat capacities for Fe-6.7 at.% Cr and Fe-21 at.% Cr alloys (b) calculated using the results of ab-initio calculations of the mixing enthalpy at 0K obtained by different authors, in comparison with the experimental data.